

## Precision Measurement of the Three $2^3P_J$ Helium Fine Structure Intervals

T. Zelevinsky,<sup>1,\*</sup> D. Farkas,<sup>1</sup> and G. Gabrielse<sup>1</sup>

<sup>1</sup>*Department of Physics, Harvard University, Cambridge, Massachusetts 02138, USA*  
(Received 20 March 2005; published 7 November 2005; corrected 11 November 2005)

The three  $2^3P$  fine structure intervals of  $^4\text{He}$  are measured at an improved accuracy that is sufficient to test two-electron QED theory and to determine the fine structure constant  $\alpha$  to 14 parts in  $10^9$ . The more accurate determination of  $\alpha$ , to a precision higher than attained with the quantum Hall and Josephson effects, awaits the reconciliation of two inconsistent theoretical calculations now being compared term by term. A low pressure helium discharge presents experimental uncertainties quite different than for earlier measurements and allows direct measurements of light pressure shifts.

DOI: 10.1103/PhysRevLett.95.203001

PACS numbers: 32.30.Bv, 31.30.Jv

This Letter reports improved measurements of the three  $^4\text{He}$   $2^3P_J$  fine structure intervals. Figure 1 shows good agreement with the most accurate measurements of three other groups, and less good agreement with two inconsistent theory values. With improved theory, the experimental accuracy is sufficient to determine the fine structure constant  $\alpha$  more precisely than can either the quantum Hall [1] or Josephson [2] effects. Only the  $\alpha$  determination from the electron magnetic moment [3] and a “preliminary” determination from Cs recoil and mass ratio measurements [4] claim smaller uncertainties. A variety of determinations is desirable for the fundamental constant that quantifies the strength of the electromagnetic interaction, and it is also attractive to determine the fine structure constant from atomic fine structure.

These intervals can be measured much more accurately than the corresponding  $2P$  intervals in H because the  $^4\text{He}$  intervals are 3 times larger, and their natural linewidths are 60 times smaller. Here, the high signal-to-noise ratio in our gas cell and the use of He pressure to vary the interaction time between atoms and light make it possible to accurately study and correct for light pressure shifts [5–9] for the first time. Measuring all three intervals [arrows in Fig. 2(a)] gives a useful internal consistency check of both the measurements and theory. Our use of magnetically resolved optical transitions in a low pressure discharge cell has very different systematic uncertainties compared to optical measurements of resolved [10] and unresolved [11] magnetic levels in a beam, and microwave measurements of resolved levels in a beam [12,13]. The most accurate measurements agree well nonetheless.

This measurement is the most stringent test of the fundamental, two-electron quantum electrodynamics (QED) calculation of He fine structure—a challenging prototype for all three-body calculations. Current theory (using  $\alpha$  from the measured electron magnetic moment and QED) disagrees with experiment on all three intervals (Fig. 1). The disagreement is similar to or a bit larger than the inconsistency between two theoretical evaluations [14,15], which should be eliminated when both groups

calculate and reconcile all of the many contributions to energy level shifts (expanded in powers of  $\alpha$  and  $\ln\alpha$ ) to order  $\alpha^7 mc^2$ . When improved theory agrees with experiment for all three fine structure intervals, our improved measurements will make it possible to deduce  $\alpha$ .

Approximately 1 in  $10^6$  of the He atoms in a continuously pumped gas cell (Fig. 3) are excited to the metastable  $2^3S_1$  state in a 60 MHz discharge. Frequency shifts due to the discharge and associated collisions are identified by varying the discharge drive power, and the He pressure (between 5 and 40 mTorr). Coils within a  $\mu$ -metal magnetic shield produce a magnetic field up to  $B = 65$  G perpendicular to the axis of the illuminated gas volume (1 cm in diameter, 15 cm long), splitting the magnetic sublevels by up to 20 linewidths.

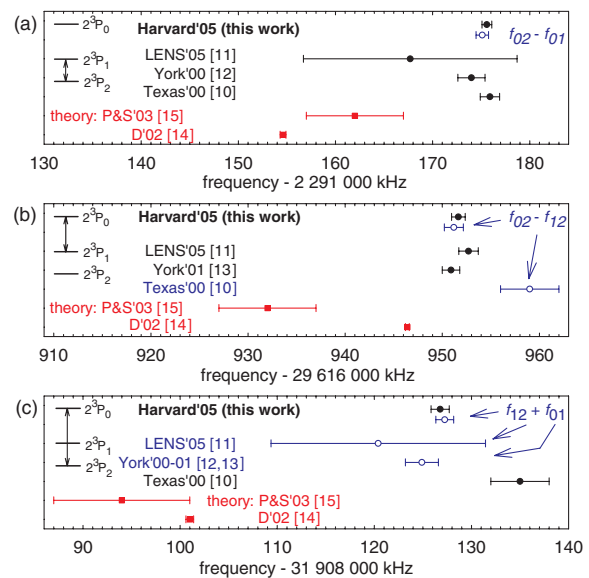


FIG. 1 (color). Most accurate measured [10–13] and calculated [14,15]  $^4\text{He}$   $2P$  fine structure intervals with standard deviations. Directly measured intervals (black filled circles) are compared to indirect values (blue open circles) deduced from measurements of the other two intervals. Uncorrelated errors are assumed for the indirect values for other groups.

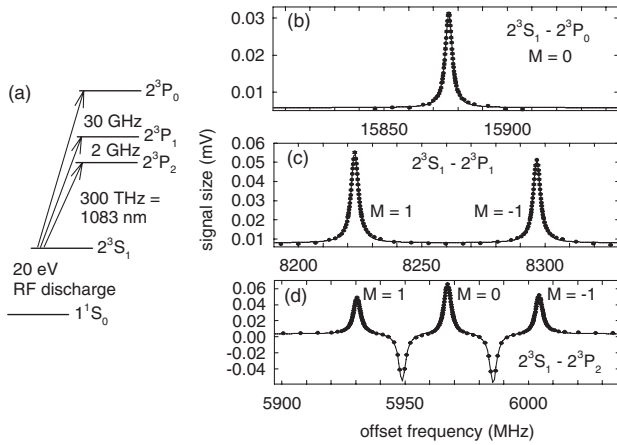


FIG. 2. Energy levels and observed transitions (arrows) are in (a), and the line shapes for each of these transitions are in (b)–(d). The probe laser transmission (points) with fits (curves) are for  $B = 52.6$  G, parallel to the pump and probe polarization axis. The two dips in (d) are crossover resonances.

Doppler-free spectroscopy of the  $2^3S_1$  to  $2^3P_J$  transitions is done with a 1083 nm diode laser (SDL-6702-H1). The diode is located within a 45 cm extended cavity to narrow its linewidth; less than 50 kHz is measured with an interferometer that has a 3 km optical fiber in one path. The light is amplified in a fiber amplifier and the light power is stabilized. The laser is split into counterpropagating and overlapping pump and probe beams, with linear polarization parallel to  $B$ . Doppler-free probe transmission is detected by a lock-in amplifier synchronously with the 35 kHz frequency of the pump chop. The pump and probe beam frequencies are offset by 2 MHz to reduce noise in the detection bandwidth. At the lowest He pressures the observed resonance widths approach the 1.6 MHz natural width.

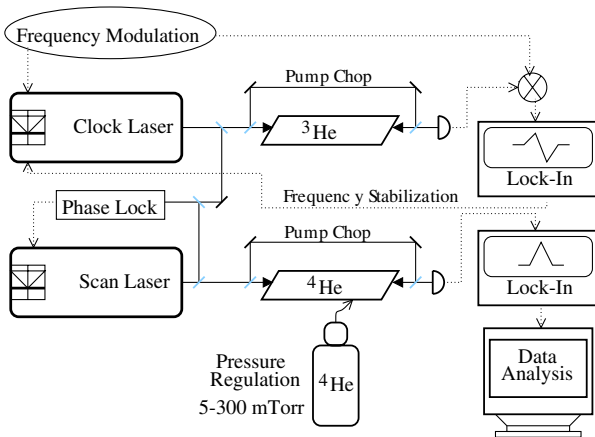


FIG. 3 (color online). Experimental setup. The 1083 nm diode “scan” laser performs saturation spectroscopy on  $^4\text{He}$ . It derives its stability from an identical “clock” laser, locked to a  $^3\text{He}$  line using frequency modulation spectroscopy.

The laser is stabilized by phase locking it to an identical reference laser which, in turn, is locked to the  $2^3S_1$  to  $2^3P_0$  ( $F, F' = 1/2$ ) transition of  $^3\text{He}$  in a fixed pressure discharge cell using frequency modulation spectroscopy. The two lasers are combined on a fast detector, and the offset frequencies are about 6, 8, and 38 GHz for the  $2^3S_1$  to  $2^3P_2$ , the  $2^3S_1$  to  $2^3P_1$ , and the  $2^3S_1$  to  $2^3P_0$  transitions of  $^4\text{He}$ . A coarse adjustment of the laser frequencies is made by varying their temperatures. The frequencies of both lasers are controlled and locked using piezos to adjust the lengths of the extended cavities, and the locking bandwidths are extended to about a MHz by adjusting the laser diode currents.

At a fixed  $B$  and  $^4\text{He}$  pressure, the change in probe transmission is measured at typically 100 different frequencies to obtain Doppler-free absorption line shapes [e.g., Figs. 2(b)–2(d)]—nearly 50 000 of which compose this data set. At 40 mTorr we measure about one resonance line shape per minute, while for 5 mTorr this takes about 5 min. The  $P_2$  line shape has the three expected absorption peaks. There are also two crossover resonances—probe transmission decreases that occur when Doppler shifts bring moving atoms in adjacent energy levels into resonance with the pump and probe beams (rather than bringing very slowly moving atoms in the same level into such resonance). The average frequency of the  $M = \pm 1$  peaks, and also that of the  $M = 0$  peak, should not be greatly shifted by crossover resonances to either side, even for an imperfect fitting model for the crossover resonances. However, the measured splitting between the  $M = \pm 1$  peaks could be so shifted, and thus is not used.

Each absorption peak [e.g., Fig. 4(a)] is a narrow Lorentzian sitting on top of a broad Gaussian background, the latter due to velocity-changing collisions (VCC) during the coherent interaction of an atom with the laser light [16–18]. For the transitions to  $P_0$  and  $P_1$  the measured fit residuals are much smaller when we fit each line to a narrow Lorentzian and the expected broad VCC Gaussian background [Fig. 4(c)] rather than to a Lorentzian and a flat background [Fig. 4(b)]. The only surprise is that the centers

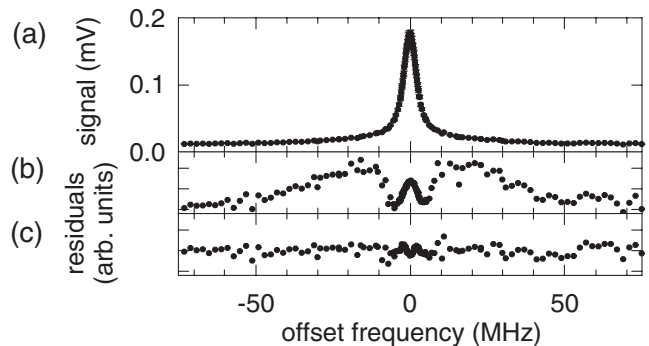


FIG. 4. Measured  $2^3S_1 - 2^3P_0$  line shape (a) gives the residuals shown for a fit to a Lorentzian plus a constant background (b) and plus a broad Gaussian background (c).

of the broad peaks are higher in frequency than the centers of the corresponding narrow peaks by approximately 5% of the width of the Gaussian background. Since the number of VCC grows with pressure, shifts from using flat rather than Gaussian backgrounds can be extrapolated to zero pressure. The slope is very small for the working pressure range under 50 mTorr, and the intercept of the differences is 0.15(11) kHz. To be safe, the intercept itself is taken to be the VCC uncertainty for  $P_0$  and  $P_1$  (even though these lines were fitted to the full line shapes) because the cause of the small frequency offset of the background Gaussians is not known. The additional resonances for  $P_2$  make it impossible to uniquely determine the broad Gaussian backgrounds. We thus fit these lines only to narrow Lorentzians with flat backgrounds, and take twice the measured intercept as a bound on the possible VCC uncertainty for intervals involving  $P_2$ .

For each interval measurement we alternate between measuring two of the three line shapes represented in Fig. 2, in an *ABBA* sequence to minimize the effect of slow drifts of our reference laser. The interval frequency is determined from the Gaussian histograms of a series of interval measurements [e.g., Fig. 5(a)] to the precision represented by the error bars in Fig. 6.

A magnetic field  $B \approx 52.6$  G along the light polarization direction resolves the energy levels. The measured linear Zeeman splitting [Fig. 5(b)] of the two  $P_1$  peaks [Fig. 2(c)], with a calculated  $B$  dependence of this shift of 1402933 Hz/G [19,20], determines the average  $\bar{B}$  for illuminated  $P_1$  atoms. The  $M = \pm 1$  splitting for  $P_2$  [Fig. 2(d)] is less reliable owing to the crossover resonances. The histogram illustrates a measured spread in  $\bar{B}$ .

The calculated and measured  $B$  for our field coils agree well when the effect of a surrounding  $\mu$ -metal shield is included. The calculations show how  $B$  varies slightly with the position from  $\bar{B}$  for the illuminated He atoms, and that corresponding distortions and shifts of the Lorentzian line shapes are too small to observe.

The measured intervals (between the center of the  $P_0$  line, and the averages of the  $M = \pm 1$  lines for  $P_1$  and  $P_2$ ) have magnetic field shifts, light pressure shifts ( $\delta$ ), and gas pressure shifts ( $a_i p$ ),

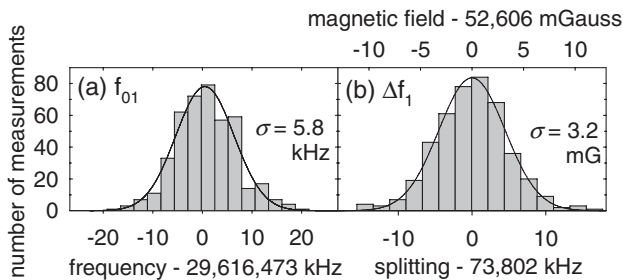


FIG. 5. Histogram for 30 h of  $f_{01}$  interval measurements (a) and for the  $2^3P_1$   $M = \pm 1$  splitting that determines  $\bar{B}$  (b).

$$\Delta f(12) = Q_{1,1} - Q_{2,1} + a_{12}p, \quad (1)$$

$$\Delta f(01) = Q_{0,0} - Q_{1,1} - \frac{1}{2}\delta + a_{01}p, \quad (2)$$

$$\Delta f(02) = Q_{0,0} - Q_{2,1} - \frac{1}{2}\delta + a_{02}p. \quad (3)$$

Linear Zeeman shifts cancel, leaving the much smaller, nonlinear Zeeman shifts  $Q_{J,|M|}$  with  $Q_{2,1} = -Q_{1,1}$ . The measured  $B$  drifts negligibly during a typical one day (e.g., Fig. 5) run, for which Zeeman corrections (e.g., Table I) are calculated with matrix elements from Ref. [20].

Light pressure shifts  $\delta$  and shifts proportional to gas pressure  $p$  [21] are also represented in Eqs. (1)–(3). An important feature of this measurement is that light pressure shifts cancel for the  $J = 1$  to  $J = 2$  interval, and are measurable for the other intervals. These shifts arise because the pump laser changes the atom velocity distribution. They are proportional to the number of photons absorbed before an atom is optically pumped into a dark state—on average two photons for our  $M = \pm 1$  transitions, three for  $J = 2$ ,  $M = 0$ , and three-halves for  $J = 0$ ,  $M = 0$ . The  $M = 0$  peak of  $P_2$  shifts by

$$\Delta = Q_{2,0} - Q_{2,1} + \delta \quad (4)$$

with respect to the average frequency of the  $M = \pm 1$  peaks. The magnetic shift calculated for a typical  $B$  is  $Q_{2,0} - Q_{2,1} = -198.12$  kHz. Measuring  $\Delta$  thus directly determines  $\delta$ , half of which is the needed light pressure correction [Eqs. (2) and (3) and Fig. 6(d)].

The open circles and statistical error bars of Fig. 6 show the measured interval shifts with gas pressure. Each is corrected for the Zeeman shift of the particular run. An uncertainty that corresponds to the maximum  $B$  drift observed over all runs is added for the  $f_{02}$  interval, for which  $B$  was not directly measured. The filled circles show the expected linear dependence after measured light pressure

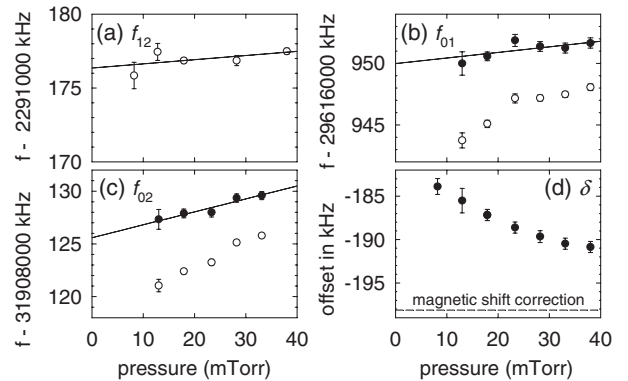


FIG. 6. Measured intervals as a function of  $^4\text{He}$  pressure  $p$  [open circles in (a)–(c)]. Offset (d) of the  $M = 0$  peak from the average of the  $M = \pm 1$  for  $P_2$  determines the light pressure shift  $\delta$ , which is then removed to get the solid dots in (b)–(c). The three intervals are then linearly extrapolated to zero  $^4\text{He}$  pressure.

TABLE I. Shifts and uncertainties that must be added to 2.291, 29.616, and 31.908 GHz, respectively.

Systematic	$f_{12}$ in kHz	$f_{01}$ in kHz	$f_{02}$ in kHz
Intercepts	176.36(37)	949.99(66)	125.58(84)
Light power	-0.96(16)	+1.20(12)	+0.78(19)
VCC	+0.00(30)	+0.00(15)	+0.00(30)
Discharge power	+0.19(09)	+0.47(12)	+0.42(24)
Typical Zeeman shift	-1188.43(00)	+471.60(00)	-716.83(00)

corrections are made. The slightly larger uncertainties for the filled points include the uncertainty in the light pressure correction. An extrapolation of the corrected values to zero gas pressure removes the effect of collisions with ground state He atoms, and any contaminant atoms, in the continuously pumped cell. The intercepts in the first line of Table I thus have shifts from  $B$ , light pressure ( $\delta$ ), and gas pressure ( $a_i p$ ) removed.

Many possible systematic shifts, such as the  $<3$  kHz second-order Doppler shift, cancel because they are the same for the optical transitions we measure. Line shifts and broadening due to curvature of the Gaussian laser wave fronts is another example. Nonetheless, we expand the laser beams up to a 2 cm diameter, keep the pump and probe powers equal, and collimate the light beam. Two observed shifts that do not cancel require extrapolation to zero discharge excitation power and to zero laser power (Fig. 7). Table I gives a summary.

The three  $2^3P$   $^4\text{He}$  fine structure intervals are

$$f_{12} = 2\,291\,175.59 \pm 0.51 \text{ kHz}, \quad (5)$$

$$f_{01} = 29\,616\,951.66 \pm 0.70 \text{ kHz}, \quad (6)$$

$$f_{02} = 31\,908\,126.78 \pm 0.94 \text{ kHz}. \quad (7)$$

Because all three intervals are measured, sums and differences provide an important consistency check (Fig. 1). The correlation coefficients for  $(f_{12}, f_{01})$ ,  $(f_{12}, f_{02})$ , and  $(f_{01}, f_{02})$  are 0.13, 0.19, and 0.73.

The three measured intervals agree well with other accurate measurements. The use of a discharge cell ensures that very different uncertainties are encountered compared to other measurements, and that light pressure shifts are

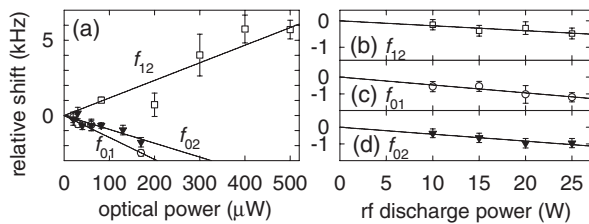


FIG. 7. Power shifts (a) and discharge shifts (b)–(d).

measured very precisely. None of the three measured intervals agrees well with two existing two-electron QED calculations, which themselves do not yet agree. The measurement accuracy is sufficient to test the expected completion and convergence of the two theoretical evaluations. These measurements and the more accurate theory should make it possible to determine  $\alpha$  to 14 ppb =  $14 \times 10^{-9}$ , a higher accuracy than attained in most other determinations. Determining the fine structure constant from atomic fine structure will provide an important check on other methods.

We are grateful to N. Hermanspahn, C. Levy, Y. Huang, T. Roach, and J. Wen for contributions to earlier versions of the experiment and to the NSF for support.

\*Present address: JILA, Boulder, CO 80309, USA.

- [1] A. M. Jeffery, R. E. Elmquist, L. H. Lee, J. Q. Shields, and R. F. Dziuba, IEEE Trans. Instrum. Meas. **46**, 264 (1997).
- [2] B. N. Taylor and E. R. Cohen, Phys. Lett. A **153**, 308 (1991).
- [3] R. S. Van Dyck, Jr., P. B. Schwinberg, and H. G. Dehmelt, Phys. Rev. Lett. **59**, 26 (1987).
- [4] A. Wicht, J. M. Hensley, E. Sarajlic, and S. Chu, Phys. Scr. **T102**, 82 (2002).
- [5] A. P. Kazantsev, G. I. Surdutovich, and V. P. Yakovlev, JETP Lett. **43**, 281 (1986).
- [6] M. G. Prentiss and S. Ezekiel, Phys. Rev. Lett. **56**, 46 (1986).
- [7] R. Grimm and J. Mlynek, Phys. Rev. Lett. **63**, 232 (1989).
- [8] M. Artoni, I. Carusotto, and F. Minardi, Phys. Rev. A **62**, 023402 (2000).
- [9] F. Minardi, M. Artoni, P. Cancio, M. Inguscio, G. Giusfredi, and I. Carusotto, Phys. Rev. A **60**, 4164 (1999).
- [10] J. Castilleja, D. Livingston, A. Sanders, and D. Shiner, Phys. Rev. Lett. **84**, 4321 (2000).
- [11] G. Giusfredi, P. de Natale, D. Mazzotti, P. C. Pastor, C. de Mauro, L. Fallani, G. Hagel, V. Krachmalnicoff, and M. Inguscio, Can. J. Phys. **83**, 301 (2005).
- [12] C. H. Storry, M. C. George, and E. A. Hessels, Phys. Rev. Lett. **84**, 3274 (2000).
- [13] M. C. George, L. D. Lombardi, and E. A. Hessels, Phys. Rev. Lett. **87**, 173002 (2001).
- [14] G. W. F. Drake, Can. J. Phys. **80**, 1195 (2002).
- [15] K. Pachucki and J. Sapirstein, J. Phys. B **36**, 803 (2003).
- [16] P. W. Smith and T. Hänsch, Phys. Rev. Lett. **26**, 740 (1971).
- [17] C. Brechignac, R. Vetter, and P. R. Berman, Phys. Rev. A **17**, 1609 (1978).
- [18] M. Pinard, C. G. Aminoff, and F. Laloë, Phys. Rev. A **19**, 2366 (1979).
- [19] M. L. Lewis and V. W. Hughes, Phys. Rev. A **8**, 2845 (1973).
- [20] Z.-C. Yan and G. W. F. Drake, Phys. Rev. A **50**, R1980 (1994).
- [21] D. Vrinceanu, S. Kotochigova, and H. R. Sadeghpour, Phys. Rev. A **69**, 022714 (2004).